Proceedings of the 17th World Congress
The International Federation of Automatic Control
Seoul, Korea, July 6-11, 2008

Sensor fusion in a Six-legged Bio-mimicking Robot

Shu-Hung Liu*, Yi-Ting Chen, Jia-Yush Yen

**Mechanical Engineering Department, National Taiwan University, Taipei10617 Taiwan (Tel: +886-2-3366-4508; e-mail: b87502061@ntu.edu.tw, jyen@ntu.edu.tw, r94522806@ntu.edu.tw)*

Abstract: This paper presents the construction of a six-legged bio-mimicking robot. The mechanical design includes the actuation design based on shape memory alloy (SMA) actuators and the locomotive mechanism. The motion control system implements various gaits for the robot to maneuver. The sensors used in the control system include the accelerometer, the compass sensor and the step sensors. We develop a sensor fusion formula to fuse the various sensor signals for enhanced position and velocity estimation. The measurement is useful for distributed information network for future robot team operation.

1. INTRODUCTION

Bio-mimicking robot has caught people's imagination for centuries. The ability of insects to deal with irregular terrain inspired engineers to build legged robots. A group of independent bio-mimicking robots could cooperate to accomplish elaborate mission. Accordingly, legged robots are very powerful for environment investigations or hazard recovery operations.

A variety of bio-mimicking walking robot has been developed in the past decades. In 1994, Dante II explored the volcano crater using a combination of supervised autonomous control and tele-operated control (Bares and Wettergreen, 1999). SCORPION was a self-contained eight-legged robot and had a distributed control system with separated control for leg reflexes (Klaassen et al., 2002). RHex uses one motor each lag to rotate the lag in full circles and to generate tripod gait using an open-loop feedforward control strategy (Saranli, Buehler and Koditschek, 2001). A bio-mimetic robot, Biobot, is physically modelled after the America cockroach and is pneumatically powered (Delcomyn and Nelson, 2000).

Shape memory alloy (SMA) actuators, on the other hand, were used in robotics since 1983. Grant and Hayward proposed designs to increase the absolute percent strain and control the non-linear effect of the SMA actuators (Grant and Hayward, 1997). Zhang et al. created a SMA micro-gripper, which was developed to assemble microscopic building blocks into tissue engineering scaffolds (Zhang et al., 2004). Stiquito is an insect-like hexapod robot propelled by nitinol actuator wires (Mills, 1993).

The underlining bio-mimicking six-legged (hexapod) robot, ROBOT III, is shown in Fig. 1. ROBOT III is actuated by the SMA actuators. The design goal is to establish an economic design for possible mass production. The robot is to have the ability to independently perform pre-assigned tasks and to make decisions when situation requires task changing. The size of ROBOT III is 20cm in length, 16.5cm in width and 9cm in height. The weight of it is 285g.

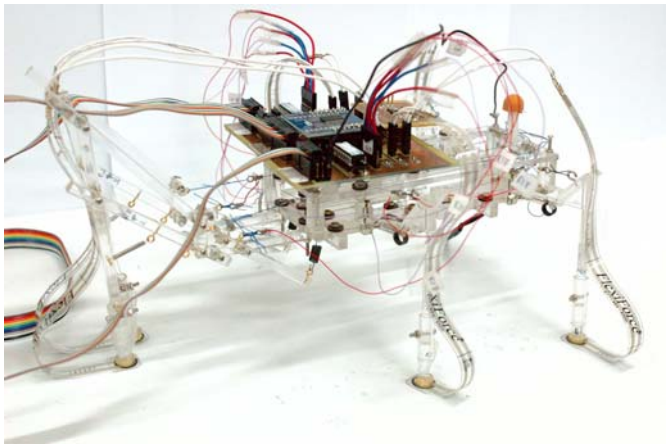

Fig. 1. ROBOT III, a SMA actuator based hexapod robot with the accelerometer, the compass sensor and the step touch sensors

The sensors used in the control system of ROBOT III include the accelerometer, the compass sensor and the step touch sensors, and sensor fusion technique is used in this study to obtain good position estimations. The idea of sensor fusion has been widely used for mobile robots (wheeled vehicles). Barshan and Durrant-Whyte proposed an inertial navigation system using extended Kalman filter (Barshan and Durrant-Whyte, 1993). Roumeliotis et al. have developed an augmenting inertial navigation system with image-based motion estimation (Roumeliotis, Johnson and Montgomery, 2002). There are few literatures about sensor fusion for legged robots. An extended Kalman filter is integrated into RHex to fuse measurements from the inertial measurement unit and a strain-gauge based leg pose sensor (Lin, Komsuoglu and Koditschek, 2006). Wijk and Christensen develop a triangular-based sonar data fusion for robot pose tracking (Wijk and Christensen, 2000). Luo et al. develop multilevel multisensor based decision fusion principles for animal robot (Luo, Phang and Su, 2001). In this study a sensor fusion formula is developed for fusing the signals from the various sensors. The sensors include the

accelerometer, the compass sensor and the step touch sensors. The proposed technique is able to provide more accurate measurement on robot position and heading.

2. HEXAPOD BIO-MIMETIC ROBOT

The hexapod bio-mimicking robot presented in the paper is ROBOT III developed in the Precision System Control Laboratory, National Taiwan University. ROBOT III is designed for autonomous operation and is based on shape memory alloy (SMA) actuators. The following subsection describes the principle of SMA actuator and ROBOT III design architecture.

2.1 Shape Memory Alloy Actuator

Shape Memory Alloy (SMA) such as TiNi alloy posses a special characteristic called Shape Memory Effect (SME). SME occurs when there is crystalline transformation between Martensite phase and Austenite phase within the alloy according to temperature change (Gorbet and Russell, 1995). This unique property makes shape memory alloys to be widely used for aeronautic applications, surgical tools, and even micro-actuators.

Table 1. Detail specifications of BMF150

	Units	Values
Standard diameter	mm	0.15
Practical force produced (load)	gf	180
Practical kinetic strain	%	4.5
Maximum contraction rate	mm/s/m	50000
Maximum elongation rate	mm/s/m	60
Service life	times	106<
Standard drive current	mA	340
Standard drive voltage	V/m	20.7
Standard power	W/m	7.05
Standard resistance	Ω/m	61
Tensile strength	kgf	1.8
Weight	mg/m	112

The SMA actuator we employed in ROBOT III is "BioMetal Fiber 150 (BMF150)" from TOKI CORPORATION. It is a fiber-like actuator designed to contract and extend like muscles. The number following BMF is the value of its diameter expressed in micrometers. The SMA actuator is a temperature-activated device. In cooled condition such as room temperature, it is soft and flexible. On the contrary, it begins to contract sharply when heated to about 70 ºC by feeding a current through it. If the passage of a current is stopped, it will soften and extend to its original length. The practical strain is 4.5% of its original length. The flexible, smooth movements make it looks like real muscle. The detail specifications of BMF150 are given in Table 1. When building a miniature robot, BMF's ultra lightweight, spacing saving characteristics provide more capability to reduce the size and weight of the robot than using motors or pneumatic actuators in traditional robot design. It can be driven at low voltage provided by batteries.

2.2 Robot Design

ROBOT III is designed based on SMA actuator. We design two sets of SMA actuators to perform body motions. One contains six SMA actuators assembled on the top plane of body to generate lifting motion in six legs. The other set has six SMA actuators assembled on the bottom plane of body to perform sweeping motion in six legs. Each SMA actuator is cooperating with a bias-spring to provide the restoring force (Elahinia and Ashrafiuon, 2002).

We use the same locomotive mechanism for front legs and middle legs. Figure 2 shows this design. The mechanism for sweeping motion is illustrated in Fig. 2. (a). When the X-directional SMA actuator is heated by a current pass through it, it contracts and pull the leg to rotate about Z-axis. When the SMA actuator is cooled, the linear spring will provide a restoring force to pull the leg back to the original position. Then the sweeping motion is generated. Figure 2 (b) shows the mechanism of lifting motion. The Z-directional SMA actuator pulls the leg to rotate about X-axis to perform the lifting motion. The torque spring provides the restoring force for the leg when the SMA actuator is cooled. Each SMA actuator is 15cm in length and is driven by 4.5V from batteries. The average power consumption for each SMA actuator is 1.5W.

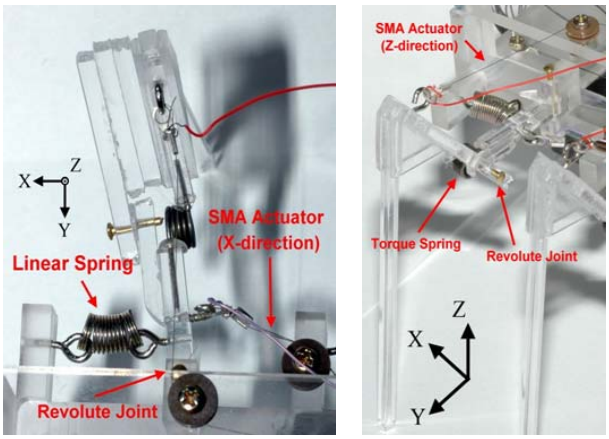

(a) (b)

Fig. 2. Locomotive mechanism for front legs and middle legs (a) The mechanism for sweeping motion, (b) The mechanism for lifting motion

The design of rear legs is different from the other legs. We assemble rear legs on the width of body instead of on the length of body such as front legs and middle legs. The installation enlarges the stable region of tripod gait. Two sets of four-bar linkages are used to produce the lifting and sweeping motion separately. Figure 3. (a) shows the mechanism for sweeping motion. NEDM is the main four-bar linkage and one SMA actuator is assembled on link MD. The rotation of link MD will generate the sweeping motion for the tip of the leg (point P). The restoring force is provided by the linear spring installed on the left side of figure. The lifting mechanism of rear leg is depicted in Fig 3 (b). The main four-bar linkage is ABCD and one SMA actuator is

assembled on link BC. The rotation of link BC will produce the lifting motion for the tip of the leg.

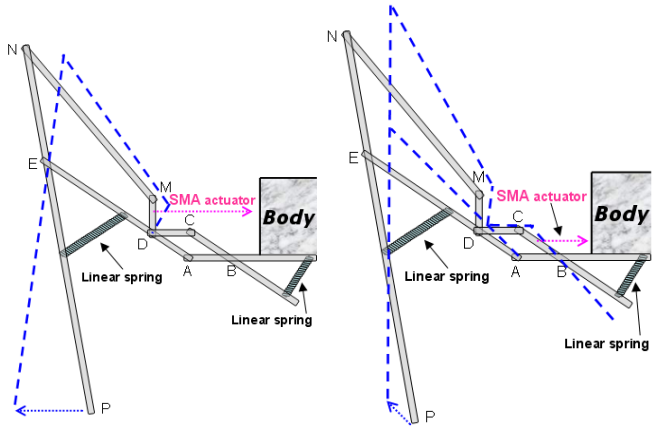

(a) (b)

Fig. 3. Locomotive mechanism for rear legs (a) The mechanism for sweeping motion, (b) The mechanism for lifting motion

3. CONTROL ARCHITECTURE

3.1 Controller

The controller of ROBOT III is A9M2410 module (see Fig. 4.), which contains a 16/32-bit RISC CPU with ARM920T core and has an embedded operating system Windows CE running on it. We develop an application on Windows CE generating gait pattern, handling data receiving from sensors, and fusing the sensing data.

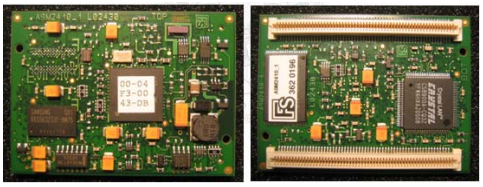

Fig. 4. A9M2410 module

3.2 Control Flow Diagram

Figure 5. shows the control flow diagram of ROBOT III. At first the controller receives the digital sensing data from compass sensor and from a 10-bit analog-to-digital converter (ADC) converting analog data from accelerometer and step touch sensors into digital values. Then the controller will generate an appropriate gait pattern based on sensor fusion results. The gait pattern generated from the I/O of the controller is send to Darlington driver IC to enlarge the current to drive the SMA actuators. The gait pattern finally performs the robot motion.

3.3 Gait Analysis

For six-legged motion, wave gaits are the most efficient and stable periodic gaits for straight motion on flat terrain (Porta and Celaya, 1998). There are four subsets of wave gaits: slow gait, crossed gait, ripple gait, and tripod gait. Furthermore, tripod gait is the fastest gait among them and is widely be used by common insect such as cockroach. Refer to Table 1, the elongation rate of SMA actuator is much slower than the contraction rate. Therefore, the walking speed of robot is mainly limited by the cooling interval of SMA actuator. Without incorporating forced cooling system, we choose the tripod gait for the following sensor fusion test.

Figure 6. illustrates the timing diagram of tripod gait pattern. The dash lines represent the retraction process that moves a leg backwards to propel the robot forward. The black bars represent the protraction process that lifts and moves the leg from the rear to the front of the robot for the next retraction (Wilson, 1966).

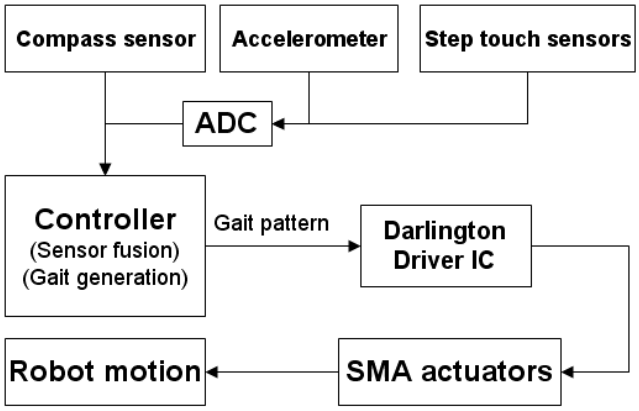

Fig. 5 Control flow diagram of ROBOT III

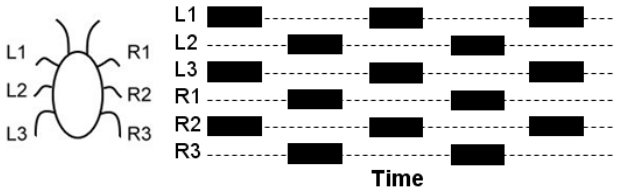

Fig. 6. Timing diagram of tripod gait pattern

4. SENSORS

In this section we give a brief description of the sensors installed on ROBOT III. A group of step touch sensors, an accelerometer, and a compass sensor provide information for the sensor data fusion process proposed in this paper. The following subsections present detailed information of these sensors.

4.1 Step Touch Sensor

A FlexiForce force sensor is integrated in each tiptoe of ROBOT III as the step touch sensor. FlexiForce force sensor is a piezoresistive sensing device in which conductance is

proportional to the applied force. The sensing force range is 1 lb (4.4N). When there is no force applied to the sensor, its resistance is very high. Conversely, resistance of the sensor is decreased when force applied to the sensor. Figure 7. shows both the force vs. resistance and force vs. conductance (1/R). Note that the conductance curve is linear, and therefore useful in calibration. We incorporate force sensor into a force-to-voltage circuit and measure the voltage by using a 10-bit analog-to-digital converter. By comparing and investigating the sensing data, we can calculate the distribution of load on the robot or distinguish from different ground textures. However, in this study we exploit the sensing data to determine whether the leg is touching the ground or not by setting a threshold voltage empirically.

The ground contact information provided by step touch sensor helped the gait controller to stabilize the gait sequence. For example, to avoid the instability condition in gait sequence such as lifting two adjacent legs simultaneously.

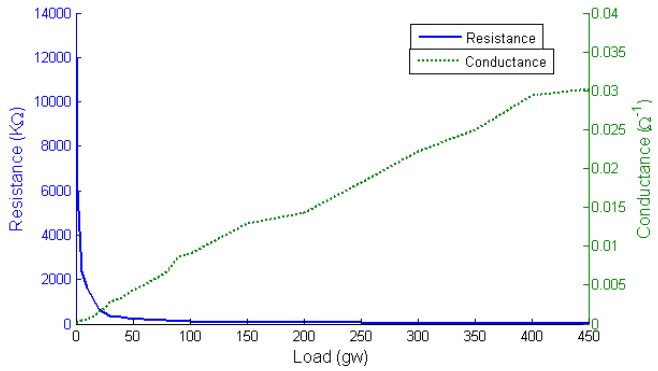

Fig. 7. Characteristics of FlexiForce force sensor

4.2 Accelerometer

An accelerometer, MEMSIC MXR2999E, is installed on the center of mass of ROBOT III. It is a dual-axis accelerometer with a measurement range of ± 0.5 g and a sensitivity of 1000 mV/g at 25 ˚C. The acceleration data are measured by a 10-bit analog-to-digital converter. The translational state component can be estimated from double integration of the accelerometer data.

4.3 Compass Sensor

Hitachi HM55B compass module is a dual-axis magnetic field sensor that provides the digital directional information. It has 6-bit (64-direction) resolution and only take 30 to 40 ms between start measurement and data-ready.

5. SENSOR FUSION

For climbing and walking legged robot, it is convenient to get the displacement information by simply calculating the number of steps then multiply by the average stride length of the gait. But in ROBOT III stride lengths may vary form step to step due to irregular terrain or the small length deviation by SMA actuators. Therefore we develop a fusion formula to mingle the stepping information from step touch sensor with the displacement data measured from double integration of the accelerometer data. The displacement fusion formula is

$$S_{K+1} = S_K + \mu_D \cdot A_K + (1-\mu_D)(\alpha_S \cdot D_S + \alpha_T \cdot D_T), \quad (1)$$

where S_{K+1} is the fusion displacement from first step to (K+1)th step, S_K is the fusion displacement from first step to Kth step, and A_K is the displacement measured from double integration of the accelerometer data within Kth step. μ_D is the weighting for displacement fusion, $0 \leqq \mu_D \leqq 1$. D_S is the average stride length when ROBOR III walks straight. Similarly, D_T is the average stride length when ROBOR III makes a turn. Note that D_S and D_T are both predetermined constant value in (1). α_S and α_T are defined as

$$\alpha_S = \begin{cases} 1 & \text{robot is walking straight} \\ 0 & \text{robot is making a turn} \end{cases},$$

and

$$\alpha_T = \begin{cases} 1 & \text{robot is making a turn} \\ 0 & \text{robot is walking straight} \end{cases}.$$

The compass sensor, as mention in section 3, could provide precise directional information. The drawback of this magnetic field sensor is that the accuracy of the sensor may decrease significantly when there are metals or magnetic fields that could contaminate the sensing signal of terrestrial magnetism near the sensor. The directional information from the compass sensor may not always accurate when the robot walks for a long distance through an unknown area; accordingly, we employ an angle fusion formula to blend the directional information from compass sensor with stepping information of the robot as

$$\theta_{K+1} = \theta_K + \mu_A \cdot C_K + (1-\mu_A) \cdot \psi, \quad (2)$$

where θ_{K+1} is the fusion angle at (K+1)th step, and θ_K is the fusion angle at Kth step. μ_A is the weighting for angle fusion, $0 \leqq \mu_A \leqq 1$. C_K is the angle value measured from compass sensor at Kth step. ψ is the average variation of angle within a step. Note that ψ is a predetermined constant value in (2).

Figure 8. shows the control flow diagram of the robot to move to the pre-assigned target position. The program begins with an angle fusion function to judge whether the robot is facing the target or not. If the robot is facing the target, the program then controls the robot to go straight. When a complete gait cycle is performed, the displacement fusion function will check if the robot arrives at the target or not. If not, the program will go back to the first stage to execute again until the robot arrives at the target. If the angle fusion function at the first stage decides the robot not to go straight, it will determine the robot to turn left or right. After a complete cycle of turning gait, the displacement fusion function will check if the robot arrives at the target or not and

decide the program should go back to the first stage or come to an end.

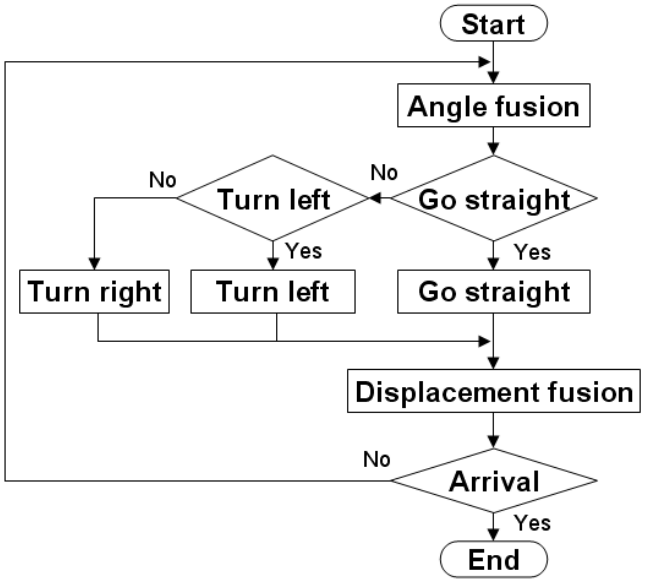

Fig. 8. Control flow diagram of robot positioning

We test the fusion program by setting the robot to face north direction at the origin as the initial condition and command the robot to go to the target position (X,Y) = (40mm, 145mm). The controller of the robot then translates the target position into target angle 15 degree (from north to east) and target displacement 150mm. Then the robot starts to move to the target position according to the information given by the sensor fusion formula. The displacement fusion result is shown in Fig. 9. During 0 to 80 seconds, the robot is making a right turn. μ_D is set to 0 and the fusion displacement only depends on stepping information. After 80 seconds, the robot stops turning and begins to walk straight. μ_D is set to 0.5 at this period. The robot arrives at the target position and stops moving at 132 seconds.

Figure 10. shows the result of angle fusion. μ_A is set to 0.8 when the robot is making a right turn during 0 to 80 seconds. Then μ_A is set to 1 when it comes to the walk straight process during 80 to 132 seconds. The target angle is 15 degree. However, we add the tolerance by setting the target angle to 15±3 degree avoiding the robot from all but making a turn.

The actual final position is (X,Y) = (33mm, 152mm). The positioning error is less the 10mm.

6. CONCLUSIONS

This paper presents the mechanical design and gait control of ROBOT III. The length of the SMA actuator is controlled using open loop control. A close-looped controller to control the length accurately will be performed in the future. The robot could perform pre-assigned tasks independently by the help of the sensor fusion formula presented in this paper. This ability is useful for future distributed information network composed by the robotic team. The authors are currently trying to develop more accurate and more efficient sensor fusion algorithm.

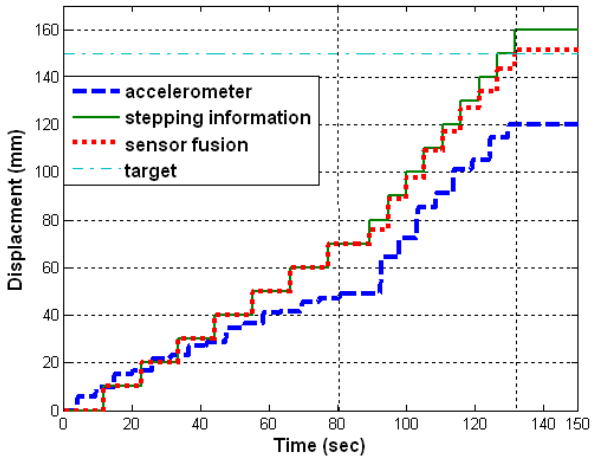

Fig. 9. The displacement fusion result

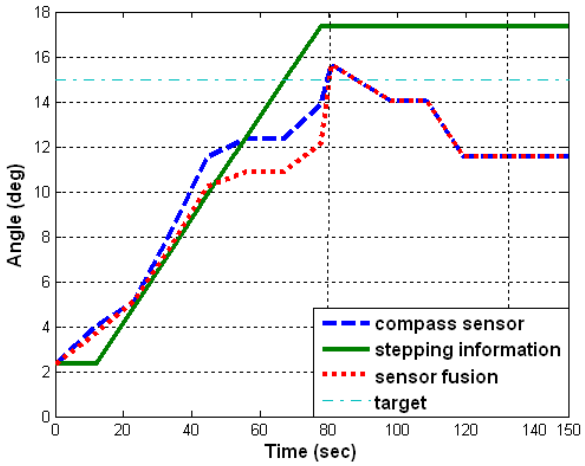

Fig. 10. The angle fusion result

REFERENCES

Bares, J. E. and D. S. Wettergreen (1999) Dante II: technical description, results, and lessons learned. *International Journal of Robotics Research,* **18,** 621-649.

Barshan, B. and H. F. Durrant-Whyte (1993) An inertial navigation system for a mobile robot. *Proceedings of the 1993 IEEE/RSJ International Conference on Intelligent Robots and Systems '93, IROS '93.*

Delcomyn, F. and M. E. Nelson (2000) Architectures for a biomimetic hexapod robot. *Robotics and Autonomous Systems,* **30,** 5-15.

Elahinia, M. H. and H. Ashrafiuon (2002) Nonlinear control of a shape memory alloy actuated manipulator. *Journal of Vibration and Acoustics, Transactions of the ASME,* **124,** 566-575.

Gorbet, R. B. and R. A. Russell (1995) Novel differential shape memory alloy actuator for position control. *Robotica,* **13,** 423-430.

Grant, D. and V. Hayward (1997) Variable structure control of shape memory alloy actuators. *IEEE Control Systems Magazine,* **17,** 80-88.

Klaassen, B., et al. (2002) Biomimetic walking robot SCORPION: Control and modeling. *Robotics and Autonomous Systems,* **41,** 69-76.

Lin, P.-C., H. Komsuoglu and D. E. Koditschek (2006) Sensor data fusion for body state estimation in a hexapod robot with dynamical gaits. *IEEE Transactions on Robotics [see also IEEE Transactions on Robotics and Automation]* **22,** 932-943.

Luo, R. C., S. H. H. Phang and K. L. Su (2001) Multilevel multisensor based decision fusion for intelligent animal robot. *Proceedings - IEEE International Conference on Robotics and Automation.* Seoul, Institute of Electrical and Electronics Engineers Inc.

Mills, J. W. (1993) Lukasiewicz insect: The role of continuous-valued logic in a mobile robot's sensors, control, and locomotion. *Proceedings of The International Symposium on Multiple-Valued Logic.* Sacramento, CA, USA, Publ by IEEE, Piscataway, NJ, USA.

Porta, J. M. and E. Celaya (1998) Gait Analysis for Six-Legged Robots. Barcelona, nstitut de Rob`otica i inform`atica Industrial.

Roumeliotis, S. I., A. E. Johnson and J. F. Montgomery (2002) Augmenting inertial navigation with image-based motion estimation. *Proceedings - IEEE International Conference on Robotics and Automation.* Washington, DC, United States, Institute of Electrical and Electronics Engineers Inc.

Saranli, U., M. Buehler and D. E. Koditschek (2001) RHex: A simple and highly mobile hexapod robot. *International Journal of Robotics Research,* **20,** 616-631.

Wijk, O. and H. I. Christensen (2000) Triangulation-based fusion of sonar data with application in robot pose tracking. *IEEE Transactions on Robotics and Automation,* **16,** 740-752.

Wilson, D. M. (1966) Insect walking. *Annual Review of Entomology,* **11,** 103-122.

Zhang, H., et al. (2004) Shape memory alloy microgripper for robotic microassembly of tissue engineering scaffolds. *Proceedings od the 2004 IEEE International Conference on Robotics and Automation, 2004 . ICRA '04.*